Jpn. J. Appl. Phys. Vol. 41 (2002) pp. 7195–7197
Part 1, No. 11B, November 2002
©2002 The Japan Society of Applied Physics

Electronic Structures of $Bi_4Ti_3O_{12}$ Thin Film and Single Crystal Determined by Resonant Soft-X-Ray Emission Spectroscopy

Tohru HIGUCHI*, Kazuhide KUDOH, Tomoyuki TAKEUCHI, Yoichiro MASUDA[1], Yoshihisa HARADA[2], Shik SHIN[2,3] and Takeyo TSUKAMOTO

Department of Applied Physics, Tokyo University of Science, Tokyo 162-8601, Japan
[1]*Department of Electrical Engineering, Hachinohe Institute of Technology, Hachinohe 031-8501, Japan*
[2]*RIKEN, Hyogo 679-5143, Japan*
[3]*Institute for Solid State Physics, University of Tokyo, Chiba 277-8581, Japan*

(Received May 29, 2002; accepted for publication June 27, 2002)

Soft-X-ray emission spectroscopy (SXES) spectra were measured for ferroelectric $Bi_4Ti_3O_{12}$ (BIT) single crystal and highly *c*-axis oriented BIT thin film. In both BIT single crystal and thin film, the Ti 3*d* and O 2*p* partial density of states (PDOS) in the valence band region were observed in O 1*s* and Ti 2*p* SXES spectra. The energy position of the Ti 3*d* state overlapped with that of the O 2*p* state, indicating the occurrence of the hybridization effect between the Ti 3*d* and O 2*p* states. The Ti 3*d* PDOS decreases in BIT thin film. This fact indicates that the hybridization effect of BIT thin film is smaller than that of BIT single crystal. [DOI: 10.1143/JJAP.41.7195]

KEYWORDS: $Bi_4Ti_3O_{12}$ (BIT), soft-X-ray emission spectroscopy (SXES), thin film, single crystal, Ti–O hybridization effect, electronic structure

1. Introduction

Bismuth layer-structured ferroelectrics such as $SrBi_2Ta_2O_9$ (SBT) and $Bi_4Ti_3O_{12}$ (BIT) consist of the layer structure of $Bi_2O_2^{2+}$ and a pseudoperovskite along the *c*-axis. In particular, BIT exhibits ferroelectricity along both the *a*- and *c*-axes.[1–3] It shows coercive fields of 3.5 kV/cm and 50 kV/cm, spontaneous polarization values of 4 μC/cm^2 and 50 μC/cm^2, and dielectric constants of 130 and 160 along the *c*- and *a*-axis, respectively. The *c*-axis-oriented BIT films are expected to be used in nonvolatile ferroelectric random access memory (FRAM) devices with nondestructive readout operation because of their low dielectric constant and coercive field along the *c*-axis. Therefore, the deposition technique of BIT thin film has been extensively investigated by sol-gel,[4,5] metalorganic chemical vapor deposition (MOCVD)[6–9] and RF magnetron sputtering methods.[10,11] Furthermore, the structural and ferroelectric properties have also been studied in the *c*-axis-oriented BIT thin films.

The fundamental structural and ferroelectric properties of BIT were studied from the 1960s to the 1970s for possible use in ferroelectric and optoelectronic devices.[1–3] However, their detailed crystal and electronic structures have not been clarified to date. In recent years, the electronic structure of the BIT thin film was studied by soft-X-ray emission spectroscopy (SXES).[12] In the valence band region, the energy position of the Ti 3*d* state overlaps with that of the O 2*p* state, indicating the occurrence of the hybridization effect between the Ti 3*d* state and O 2*p* state. The hybridization effect is also expected based on the result of the band calculation, in which optimized basis sets with effective core potentials are used. In the case of band calculation, Shimakawa *et al.*[13] reported that the covalent interaction, which originates from the strong hybridization effect between Ti 3*d* and O 2*p* states, plays an important role in the structural distortion and ferroelectricity of the BIT material. Thus, we believe that the hybridization effect of the BIT thin film is different from that of the BIT single crystal.

In the present study, the electronic structures of BIT single crystal and BIT thin film have been investigated by SXES. It is known that the SXES technique can enable investigation of the electronic structure of the bulk state unlike the photoemission spectra, because the mean free path of a soft-X-ray is very long compared with that of an electron.[14] Furthermore, the electronic structure of an insulating material can also be measured by SXES. On the other hand, the partial density of states (PDOS) localized at the atom can be obtained from SXES spectra, because the SXES has a clear selection rule regarding the angular momentum due to dipole selection.[14–18] In order to study the hybridization effects of the BIT single crystal and the BIT thin film, we measured the SXES spectra in the energy regions of Ti 2*p* and O 1*s* excitation thresholds.

2. Experimental

A BIT thin film was deposited on a Pt/Ti/SiO_2/Si substrate by the RF magnetron sputtering method with Bi_2O_3 and TiO_2 ceramic targets. When the RF powers applied to Bi_2O_3 and TiO_2 targets are 200 W and 100 W, respectively, the obtained BIT thin films have the stoichiometric composition. For the deposition of BIT thin film, an operating pressure of 10 mTorr was maintained during deposition. The total gas pressure of Ar and O_2 was 10 mTorr. The substrate temperature was maintained at about 600°C. The film thickness was about 400 nm. The X-ray diffraction (XRD) pattern of the thin film clearly exhibits a highly *c*-axis-oriented BIT single phase, which has no pyrochlore phase of $Bi_2Ti_2O_7$. Then, the remanent polarization and coercive field were 4.09 μC/cm^2 and 56.1 kV/cm, respectively. The dielectric constant was about 330. The detailed ferroelectric and structural properties have previously been reported in ref. 11).

BIT single crystal was grown by the flux method. The XRD pattern of the single crystal exhibited the BIT single phase. Then, the remanent polarization and coercive field were 4.10 μC/cm^2 and 5.1 kV/cm, respectively. The dielectric constant was about 140.

*E-mail address: higuchi@rs.kagu.tus.ac.jp

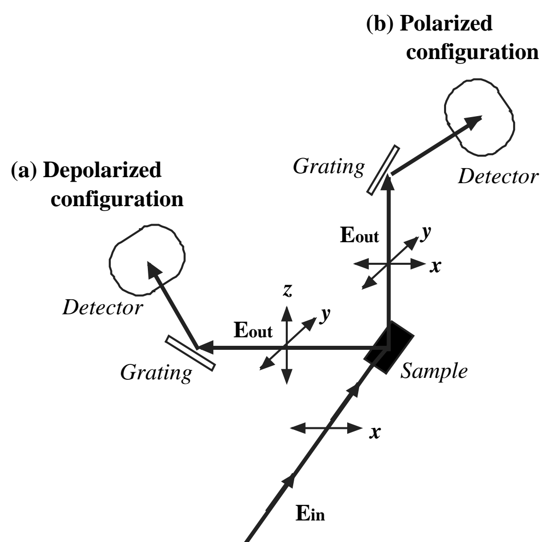

Fig. 1. Schematic diagrams of (a) depolarized and (b) polarized configurations for SXES. (a) Depolarized configuration: the spectrometer is located in the direction of the polarization vector of the incident photon (E_{in}). (b) Polarized configuration: the spectrometer is located normal to the wave vector and the polarization vector of E_{in}.

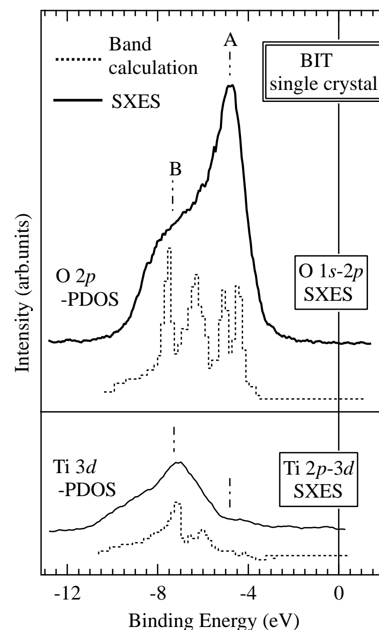

Fig. 2. O 1s and Ti 2p SXES spectra of BIT single crystal. As reference, the calculated band DOS is also shown under each SXES spectrum.

SXES spectra were measured using a soft-X-ray spectrometer installed at the undulator beamline BL-2C (in Photon Factory) at the High Energy Accelerator Organization. Synchrotron radiation was monochromatized using a varied-line spacing plain grating whose average groove density was 1000 lines/mm. The energy resolution was about 0.4 eV at $h\nu = 450$ eV.

Figure 1 shows a schematic diagram of the experimental system. In this study, the SXES spectra were measured at the polarized configuration. As a reference, the depolarized configuration is also shown in this figure.[16] In the depolarized configuration, the polarization vector of the emitted photon (E_{out}) is rotated by 90° from the polarization vector of the incident photon (E_{in}). In the polarized configuration, the polarization vector of E_{out} contains the same polarization vector as that of E_{in}. Therefore, the SXES spectra at the polarized configuration reflect the electronic structure within the *a*-*b* plane.

3. Results and Discussion

Figure 2 shows the valence band by the O 1s and Ti 2p SXES of a BIT single crystal. The O 1s SXES spectrum measured at $h\nu = 550$ eV reflects the O 2p PDOS. The Ti 2p SXES spectrum measured at $h\nu = 500$ eV reflects the Ti 3d PDOS. It is striking that the energy position of the O 2p state overlaps that of the Ti 3d state in the valence band. The valence band has two features, A and B, at 5.2 and 8.3 eV, respectively. Comparing each PDOS, the Ti 3d contribution is more significant in the higher energy region (feature B), where the O 2p states have a larger admixture of the Ti 3d state. This shows that the indispensable magnitudes mix with the valence states. In other words, the valence states originating from the O 2p states are hybridized with the Ti 3d state. Therefore, we can estimate that the features arising from the bonding states occur at a higher binding energy (feature B) and those from the nonbonding states occur at a lower binding energy (feature A).[12]

As a reference, the calculated PDOS is also shown under each SXES spectrum in Fig. 2. The electronic structure calculations based on the density functional theory using local density approximation (LDA) were performed using the *ab-initio* calculation program. To calculate the electronic structure, we optimized the basis sets with effective core potential. The calculated PDOS curves are obtained by convoluting the original PDOS with Gaussian broadening functions with the width of 0.5 eV, which corresponds to the total resolution of the experimental system. The calculated O 2p PDOS has four peaks, which correspond to Γ, X, P and N points in the tetragonal Brillouin zone. The O 1s SXES spectrum also shows the two peaks, A and B (nonbonding and bonding peaks). Although the intensities of nonbonding and bonding peaks in the O 1s SXES spectrum are different from the calculated O 2p PDOS, the reason for this has not been clarified thus far. The bandwidths of calculated PDOS are in good accordance with those of the Ti 2p and O 1s SXES spectra.

Figure 3 shows the comparison of the O 2p PDOS and Ti 3d PDOS in the valence band between the BIT single crystal and BIT thin film. The solid line and dashed line indicate BIT thin film and single crystal, respectively. The intensities of the SXES spectra are normalized by beam current and measurement time. By this normalization, it is evident that the intensity of the elastic scattering in the BIT single crystal is in good agreement with that in the BIT thin film. It is clear that the O 2p state of BIT thin film hybridizes with the Ti 3d state in the valence band, as shown in the case of the BIT single crystal of Fig. 2. The bandwidths of O 2p and Ti 3d states in the BIT thin film are in good agreement with those in BIT single crystal. The intensity of the Ti 3d PDOS in the BIT thin film is lower than that in the BIT single crystal, indicating that the hybridization effect between the Ti 3d and O 2p states is smaller in the case of the BIT thin film. On the other hand, the change of O 2p PDOS is smaller than that of Ti 3d PDOS. The reason for this is considered to be due to

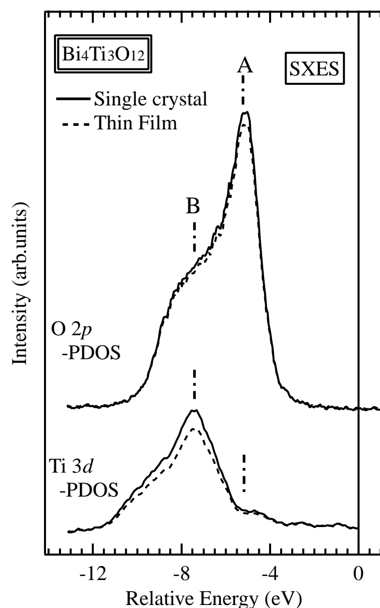

Fig. 3. Comparison of the SXES spectra between BIT single crystal (solid line) and BIT thin film (dashed line). Features A and B indicate the non-bonding state and bonding state, respectively.

the oxygen deficiency of the BIT thin film.

In recent years, the electronic structure of ferroelectric $BaTiO_3$ was measured by resonant photoemission spectroscopy (RPES).[19–21] From the RPES study,[19] it has been clarified that the O $2p$ state of $BaTiO_3$ hybridizes with the Ti $3d$ state in the valence band. The hybridization effect between the Ti $3d$ and O $2p$ states in the ferroelectric phase is lower than that in the paraelectric phase. This fact can be explained by the change of the bond length between Ti and O ions.[19] Such a situation might also be expected in the BIT single crystal and thin film. The lattice parameters of BIT single crystal were $a = 5.41$ Å, $b = 5.45$ Å and $c = 32.83$ Å. The lattice parameters of BIT thin film were $a = 5.43$ Å, $b = 5.45$ Å and $c = 32.82$ Å. Therefore, the lattice parameter along the a-axis is larger in the BIT thin film, indicating the increase of the bond length between Ti an O ions.

4. Conclusions

We have studied the difference of the electronic structure between BIT single crystal and BIT thin film by SXES. In both BIT single crystal and BIT thin film, the O $2p$ state hybridizes with the Ti $3d$ state in the valence band. The hybridization effect between the O $2p$ state and Ti $3d$ state is weaker in the BIT thin film. This fact is considered to originate in the increase of the bond length between Ti and O ions within the a–b plane.

Acknowledgements

We would like to thank Professor S. Okamura and Dr. H. Kakemoto for helpful discussions. This work was partly supported by the Foundation for Promotion of Material Science and Technology of Japan (MST Foundation), and a Grant-In-Aid for Science Research (No. 13740191) from the Ministry of Education, Culture, Sports, Science and Technology of Japan.

1) E. C. Subbarao: Phys. Rev. **122** (1961) 804.
2) S. E. Cummins and L. E. Cross: Appl. Phys. Lett. **10** (1967) 14.
3) R. W. Wolfe and R. E. Newnham: J. Electrochem. Soc. **116** (1967) 832.
4) A. Kakimi. S. Okamura and T. Tsukamoto: Jpn. J. Appl. Phys. **33** (1994) L1707.
5) S. Okamura, Y. Yagi, K. Mori, G. Fujihashi, S. Ando and T. Tsukamoto: Jpn. J. Appl. Phys. **36** (1997) 5889.
6) T. Tsukamoto and S. Okamura: Ferroelectrics **170** (1995) 77.
7) R. Muhammet, T. Nakamura, M. Shimizu and T. Shiosaki: Jpn. J. Appl. Phys. **33** (1994) 5215.
8) T. Kijima and H. Matsunaga: Jpn. J. Appl. Phys. **37** (1998) 5171.
9) M. Yamaguchi and T. Nagatomo: Thin Solid Films **348** (1999) 294.
10) Y. Masuda, H. Masumoto, A. Baba, T. Goto and T. Hirai: Jpn. J. Appl. Phys. **32** (1993) 4043.
11) M. Tanaka, T. Higuchi, K. Kudoh and T. Tsukamoto: Jpn. J. Appl. Phys. **41** (2002) 1536.
12) T. Higuchi, M. Tanaka, K. Kudoh, T. Takeuchi, S. Shin and T. Tsukamoto: Jpn. J. Appl. Phys. **40** (2001) 5803.
13) Y. Shimakawa, Y. Kubo, Y. Taguchi, H. Asano, T. Kamiyama, F. Izumi and Z. Hiroi: Appl. Phys. Lett. **79** (2001) 2791.
14) S. Shin, A. Agui, M. Watanabe, M. Fujisawa and T. Ishii: J. Electron Spectrosc. Relat. Phenom. **79** (1996) 125.
15) Y. Tezuka, S. Shin, A. Agui, M. Fujisawa and T. Ishii: J. Phys. Soc. Jpn. **65** (1996) 312.
16) Y. Harada, T. Kinugasa, R. Eguchi, M. Matsubara, A. Kotani, M. Watanabe, A. Yagishita and S. Shin: Phys. Rev. B **61** (2000) 12854.
17) T. Higuchi, T. Tsukamoto, M. Watanabe, M. M. Grush, T. A. Callcott, R. C. Perera, D. L. Ederer, Y. Tokura, Y. Harada, Y. Tezuka and S. Shin: Phys. Rev. B **60** (1999) 7711.
18) T. Higuchi, T. Tsukamoto, M. Watanabe, Y. Harada, Y. Tezuka, Y. Tokura and S. Shin: Physica B **281&282** (2000) 615.
19) T. Higuchi, T. Tsukamoto, K. Oka, T. Yokoya, Y. Tezuka and S. Shin: Jpn. J. Appl. Phys. **38** (1999) 5667.
20) T. Higuchi, T. Tsukamoto, N. Sata, M. Ishigame, Y. Tezuka and S. Shin: Phys. Rev. B **57** (1998) 6978.
21) T. Higuchi, T. Tsukamoto, S. Yamaguchi, Y. Tezuka and S. Shin: Jpn. J. Appl. Phys. **40** (2001) L201.